



King Saud University

Arabian Journal of Chemistry

www.ksu.edu.sa  
www.sciencedirect.com



ORIGINAL ARTICLE

# Theoretical study of fMet-tRNA and fAla-tRNA structures by using quantum calculation



M. Noei <sup>a</sup>, A. A. Salari <sup>b</sup>, Mohammad T. Baei <sup>c,\*</sup>, F. Hajizadeh <sup>b</sup>,  
Jamal Kazemi Asl <sup>d</sup>, Mohammad Ramezani Taghartapeh <sup>e</sup>

<sup>a</sup> Department of Chemistry, Mahshahr Branch, Islamic Azad University, Mahshahr, Iran

<sup>b</sup> Department of Chemistry, Shahre Rey Branch, Islamic Azad University, Tehran, Iran

<sup>c</sup> Department of Chemistry, Azadshahr Branch, Islamic Azad University, Azadshahr, Golestan, Iran

<sup>d</sup> Faculty of Science, Payame Noor University (PNU), Bandar Imam Khomeini, Iran

<sup>e</sup> Young Researchers Club, Gorgan Branch, Islamic Azad University, Gorgan, Iran

Received 5 September 2011; accepted 22 November 2011

Available online 29 November 2011

KEYWORDS

fMet-tRNA;  
fAla-tRNA;  
DFT;  
NBO;  
NMR

**Abstract** In the prokaryotes, protein synthesis always starts with N-formylmethionine amino acid. Comparison of this amino acid with other amino acids is attempted and that is why formylmethionine is always the first amino acid to begin protein synthesis, in this paper we added a formyl group to alanine amino acid and then studied it when attached to the tRNA molecule and compared this structure with formylmethionine-tRNA structure. The quantum chemical calculations have performed using Gaussian 03 suite of programs. The fAla-tRNA and fMet-tRNA structures have fully optimized at the HF and B3LYP levels with 3-21G\* and 6-31G\* basis sets as well as MP2/3-21G\* level and theoretically solvent effects on the structures were investigated. Then we studied electronic structures of the compounds using Natural Bond Orbital (NBO) analysis and calculated NMR parameters at the gas-phase. Frequency analysis was also calculated at the HF and B3LYP/3-21G\* levels in the different solvents in 298.15 K, 310.15 K temperatures and 1.00 atmosphere pressure.

© 2011 Production and hosting by Elsevier B.V. on behalf of King Saud University. This is an open access article under the CC BY-NC-ND license (<http://creativecommons.org/licenses/by-nc-nd/3.0/>).

## 1. Introduction

In the prokaryotes, proteins are synthesized starting with N-formylmethionine amino acid. The initiation codon is most

often 5'-AUG-3' (Less often, the initiation codon is 5'-GUG-3' or 5'-UUG-3') (Chamieh et al., 2008; Chalut and Egly, 1995). N-formylmethionine and methionine are coded by the same AUG codon. When the AUG codon is used for initiation, initiator tRNA only recognizes N-formylmethionine instead of methionine. The N-terminal methionine residue of bacterial proteins is post-translationally modified to N-methyl-methionine (Yu Wang et al., 2002). Before formyl group attached to amino group of methionine, it first attached to tRNA molecule. Formylmethionine is brought to the ribosomal P site by an initiator tRNA to start protein synthesis. Once translation is com-

\* Corresponding author. Tel.: +98 9111751399.

E-mail address: [Baei52@yahoo.com](mailto:Baei52@yahoo.com) (M.T. Baei).

Peer review under responsibility of King Saud University.



Production and hosting by Elsevier

plete, peptide deformylase removes the formyl group from fMet (Spector et al., 2003; Tang et al., 2004).

The bacterial ribosome is composed of two subunits. Together the large and small subunits form a 70S ribosome (Laursen et al., 2005; Selmer et al., 2006; Yusupov et al., 2001; Baouz et al., 2009; Agirrezabala and Frank, 2009). The larger 50S ribosomal subunit and the smaller 30S subunit create the peptidyl (P) site, aminoacyl (A) site, and exit (E) site (Feinberg and Joseph, 2006; Trabuco et al., 2010; Munro et al., 2009; Carter et al., 2000). Bacterial protein synthesis starts through the pre-initiation complex that is composed of the 30S subunit, mRNA, initiator transfer RNA charged with formylmethionine (fMet-tRNA), GTP and three protein initiation factors: IF1, IF2 and IF3. This complex then binds to the 50S subunit, forming the 70S ribosome (Pavlov et al., 2008; Wienk et al., 2005). During the first elongation step, fMet-tRNA is already positioned in the ribosomal P site. After initiation, once an aa-tRNA is delivered to the ribosomal A site with elongation factor-Tu (EF-Tu) and GTP, a peptide bond forms between fMet and the A-site amino acid (Trabuco et al., 2010; Carter et al., 2000). tRNA is a small RNA molecule containing about 70–90 nucleotides. Each tRNA molecule is able to recognize the codons triplet from mRNA, and then tRNA carries out the respective amino acid to the protein-building machinery. In order to add amino acid successfully, the tRNA has to read the coded segment accurately from mRNA (Chuang et al., 2010). If a 50S subunit docks to a 30S subunit in complex with an elongator, rather than with the initiator tRNA, this may lead to the synthesis of a protein with an aberrant N-terminal amino acid sequence or to out-of-frame mRNA reading. It is therefore essential that the initiator tRNA, rather than an elongator tRNA, binds to the mRNA-programmed 30S subunit and eventually becomes P site bound in the 70S initiation complex (Antoun et al., 2006). The issue addressed in this study is what is the difference between the initiator tRNA (fMet-tRNA) and other aa-tRNAs that makes it only be reasonable for initiation of protein synthesis. In this paper we selected alanine amino acid that is coded by GCU, GCC, GCA, and GCG. Alanine is a non-Polar compound as methionine that has simplest structure of methionine. We added a formyl group to alanine using Gaussian 03 suite of programs and then studied when attached to the proper tRNA molecule (Fig. 2) and compared this structure with formylmethionine-tRNA structure (Fig. 1). tRNA molecule by 3'-CCA end of acceptor stem is linked to an amino acid. For simplifying the computations, we only worked with adenine nucleotide as tRNA.

## 2. Computational details

The quantum chemical calculations were performed using Gaussian 03 suite of programs (Frisch and et al., 2003). The structures of fAla-tRNA and fMet-tRNA have been fully optimized at the HF and B3LYP levels with 3-21G\*, 6-31G\* basis sets and MP2/3-21G\* level and theoretically were investigated solvent effects using the Onsager reaction field model. In the Onsager model, solute whose charge distribution is represented by a simple dipole, is embedded in a typically fixed spherical cavity (LaPlante and Stidham, 2009) and interacts with the solvent (Szarecka et al., 1998). In this model, Gas-phase geometry is first optimized with a level of theory then the recommended

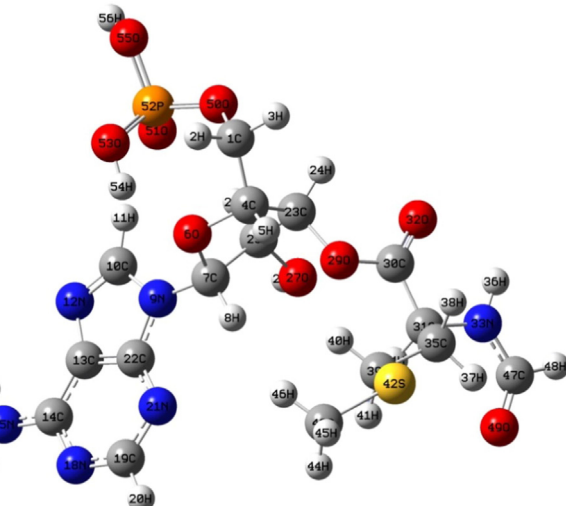


**Figure 1** Structure of fMet with adenine.

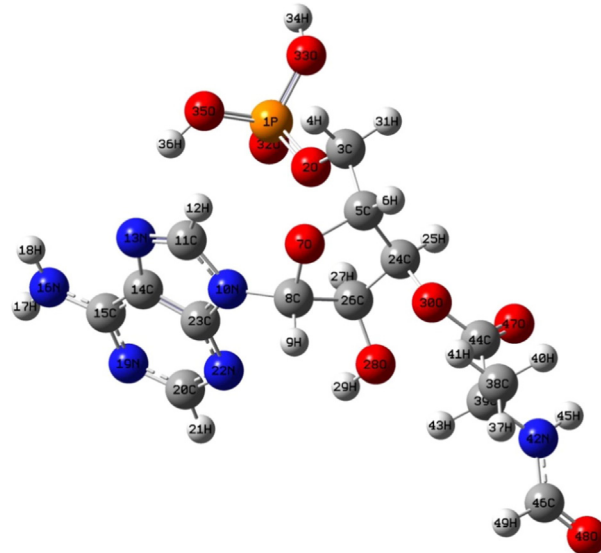


**Figure 2** Structure of fAla with adenine.

cavity radius for the SCRF calculation is obtained from single point calculations using a Volume keyword (Nekoei et al., 2009; Blicharska and Kupka, 2002; Giese and McNaughton, 2002) finally, the self consistent reaction field (SCRF) calculations with SCRF = Dipole keyword (Blicharska and Kupka, 2002; Giese and McNaughton, 2002) are performed at the same level of theory. In the SCRF theory, the solvent is considered as a uniform field of dielectric constant  $\epsilon$ . The solute is assumed to occupy a spherical cavity of radius ( $a_0$ ) in the solvent (Nandini and Sathyaranayana, 2004).

We also studied electronic structures of compounds using Natural Bond Orbital (NBO) analysis at the same levels that were mentioned above in the different solvents and calculated NMR parameters at the gas-phase. So frequency at the HF/3-21G\* and B3LYP/3-21G\* levels in the various solvents in 298.15 K, 310.15 K temperatures and 1.00 atmosphere pressure was calculated.

A generally applied tool for the quantification of hyperconjugative interactions is the natural bond orbital method (NBO) (Wedel et al., 2008). NBO analysis is based on a method for optimal transformation of a given wavefunction into a localized form, corresponding to the one-center (“lone pair”) and two-center (“bond”) elements of the Lewis structure picture (Scholtzová et al., 2009). The NBOs are one of a sequence of natural localized orbital sets that include natural atomic (NAO), hybrid (NHO), and (semi-)localized molecular orbital (NLMO) sets, intermediate between basis AOs and canonical molecular orbitals (Mos). Each of these localized sets is complete and orthonormal (Weinhold and Landis, 2001; Alabugin et al., 2003). Energies of the corresponding orbitals are the expectation values (diagonal matrix elements) of the Fock or Kohn-Sham operator (Alabugin et al., 2003).

### 3. Results and discussion

#### 3.1. Geometry optimization

Structures of fAla-tRNA and fMet-tRNA in gas phase, DMSO, CHCl<sub>3</sub>, and H<sub>2</sub>O solvents, with relative dielectric constants  $\mathcal{E} = 46.7$ , 4.9 and 78.39 respectively (Aquino et al., 2002), optimized at the HF, B3LYP and MP2 levels of theory. Relative energies have been presented in Table 1.

The calculated results in Table 1 showed that the relative energy for fMet-tRNA in the methods is more than that of fAla-tRNA that represents fMet-tRNA structure that is more stable.

#### 3.2. NBO analysis

Natural bond orbital analysis provides the accurate possible natural Lewis structure picture of  $\psi$ , because all orbital details are mathematically chosen to include the highest possible percentage of the electron density (Weinhold and Landis, 2001; Subashchandrabose et al., 2010). The result of interaction is a loss of occupancy from the concentration of electron NBO of the idealized Lewis structure into an empty non-Lewis orbital. A careful examination of all possible interactions between “filled” (donor) Lewis-type NBOs and “empty” (acceptor) non-Lewis NBOs, allows us to get an estimate of their energetic importance by second-order perturbation theory. For each donor ( $i$ ) and acceptor ( $j$ ), the stabilization energy  $E^{(2)}$  associates with the delocalization  $i \rightarrow j$  is estimated as:

$$E^{(2)} = \sum E_{ij} = q_i(F(i,j)^2)/(\epsilon_j - \epsilon_i) \quad (1)$$

where  $q_i$  is the donor orbital occupancy,  $\epsilon_j$  and  $\epsilon_i$  are diagonal elements and  $F(i,j)$  is the off diagonal NBO Fock matrix element (Subashchandrabose et al., 2010; Jayabharathia et al., 2010a,b; Krishnan et al., 2010). According to the simple bond orbital picture, each bonding NBO is defined as an orbital formed from two directed valence hybrids (NHOs)  $h_A$ ,  $h_B$  on atoms  $A$  and  $B$ , with corresponding polarization coefficients  $c_A$ ,  $c_B$ :

$$\sigma_{AB} = c_A h_A + c_B h_B \quad (2)$$

To complete the span of the valence space, each valence bonding NBO must in turn be paired with a corresponding valence antibonding NBO (Weinhold and Landis, 2001)

$$\sigma_{AB^*} = c_B h_A - c_A h_B \quad (3)$$

We noted results of natural atomic hybrids (NHOs) on three atoms in link area with the polarization coefficient  $c_A$ ,  $c_B$  for each method in the corresponding NBO. Tables 2 and 3 show these studies for fMet-tRNA and fAla-tRNA using the selected methods.

The next section shows some of the donor–acceptor interactions and their second order perturbation energies ( $E^{(2)}$ ) for two compounds. The results of the NBO analysis in Tables 4 and 5 show that in fMet-Adenine link from fMet-tRNA structure, LP(2)O<sub>32</sub> participates as donor and the  $\sigma^*(O_{29}-C_{30})$  interactions as acceptor in hyperconjugative interactions and in fAla-Adenine link from fAla-tRNA structure, LP(2)O<sub>47</sub> participates as donor and the  $\sigma^*(O_{30}-C_{44})$  interactions as acceptor in hyperconjugative interactions. Electron density is transferred from Chojnacki (2008) one pair LP(2) O<sub>32</sub> to the anti-bonding  $\sigma^*(O_{29}-C_{30})$  orbital's in fMet-tRNA and LP(2)O<sub>47</sub> to the anti-bonding  $\sigma^*(O_{30}-C_{44})$  orbital's in fAla-tRNA.

The resonance energy ( $E^{(2)}$ ) indicates amount of Participation of electrons in the resonance here, its value in the gas phase is more than that in the solvent that indicates more electrons' participation in the resonance of the connection area in this phase and among the solvents for fMet-tRNA, in DMSO, and for fAla-tRNA, in CHCl<sub>3</sub>, more electrons are involved in the resonance.

The population analysis represents determination of the distribution of electrons in a molecule, creating orbital shapes and derivation of atomic charges and dipole moments. The Natural Population Analysis (NPA) is a more refined wave function-based method that solves most of the problems of the Mulliken scheme by construction of a more appropriate set of (natural) atomic basis functions (Martin and Zipse, 2005). Table 5 shows the atomic charge distribution in terms of NPA charges for the selected compounds.

Natural Population Analysis (NPA) seems to exhibit improved numerical stability and gives a better description of

**Table 1** Relative energy (kcal/mol) of the fMet-tRNA and fAla-tRNA structures.

Method	fMet-tRNA				fAla-tRNA			
	Gas	CHCl <sub>3</sub>	DMSO	H <sub>2</sub> O	Gas	CHCl <sub>3</sub>	DMSO	H <sub>2</sub> O
HF/3-21G*	0.00	0.00	0.00	0.00	0.00	0.00	0.00	0.00
HF/6-31G*	-12.42	-12.42	-12.42	-12.42	-10.15	-10.15	-10.15	-10.15
B3LYP/3-21G*	-15.62	-15.62	-15.62	-15.62	-14.38	-14.38	-14.38	-14.38
B3LYP/6-31G*	-23.02	-23.02	-23.02	-23.02	-19.51	-19.51	-19.51	-19.51
MP2/3-21G*	-28.35	-28.35	-28.35	-28.35	-28.04	-28.04	-28.04	-28.04

**Table 2** Calculated NHOs and the polarization coefficient for each hybrid in the corresponding NBO (in parentheses) for fMet-tRNA.

Phase	Method	C <sub>30</sub> —O <sub>29</sub>		C <sub>30</sub> —O <sub>32</sub>		C <sub>30</sub> —O <sub>32</sub>	
		C <sub>30</sub>	O <sub>29</sub>	C <sub>30</sub>	O <sub>32</sub>	C <sub>30</sub>	O <sub>32</sub>
Gas	HF/3-21G*	sp <sup>2.66</sup> (0.5472)	sp <sup>1.93</sup> (0.8370)	sp <sup>2.07</sup> (0.5732)	sp <sup>1.26</sup> (0.8194)	sp <sup>1.00</sup> (0.5433)	sp <sup>1.00</sup> (0.8396)
	B3LYP/3-21G*	sp <sup>2.64</sup> (0.5602)	sp <sup>2.19</sup> (0.8283)	sp <sup>2.12</sup> (0.5811)	sp <sup>1.56</sup> (0.8138)	sp <sup>99.99</sup> (0.5660)	sp <sup>99.99</sup> (0.8244)
	MP2/3-21G*	sp <sup>2.68</sup> (0.5546)	sp <sup>2.27</sup> (0.8321)	sp <sup>2.06</sup> (0.5794)	sp <sup>1.53</sup> (0.8151)	sp <sup>99.99</sup> (0.5290)	sp <sup>99.99</sup> (0.8487)
	HF/6-31G*	sp <sup>2.48</sup> (0.5462)	sp <sup>1.83</sup> (0.8377)	sp <sup>1.98</sup> (0.5751)	sp <sup>1.19</sup> (0.8181)	sp <sup>99.99</sup> (0.5054)	sp <sup>99.99</sup> (0.8629)
	B3LYP/6-31G*	sp <sup>2.52</sup> (0.5538)	sp <sup>2.00</sup> (0.8327)	sp <sup>2.02</sup> (0.5811)	sp <sup>1.38</sup> (0.8138)	sp <sup>99.99</sup> (0.5401)	sp <sup>99.99</sup> (0.8416)
CHCl <sub>3</sub>	HF/3-21G*	sp <sup>2.65</sup> (0.5477)	sp <sup>1.94</sup> (0.8367)	sp <sup>2.07</sup> (0.5731)	sp <sup>1.26</sup> (0.8195)	sp <sup>1.00</sup> (0.5445)	sp <sup>1.00</sup> (0.8387)
	B3LYP/3-21G*	sp <sup>2.64</sup> (0.5605)	sp <sup>2.20</sup> (0.8281)	sp <sup>2.12</sup> (0.5813)	sp <sup>1.57</sup> (0.8137)	sp <sup>99.99</sup> (0.5665)	sp <sup>99.9</sup> (0.8241)
	MP2/3-21G*	sp <sup>2.68</sup> (0.5563)	sp <sup>2.39</sup> (0.8310)	sp <sup>2.09</sup> (0.5775)	sp <sup>1.58</sup> (0.8164)	sp <sup>1.00</sup> (0.5797)	sp <sup>99.99</sup> (0.8148)
	HF/6-31G*	sp <sup>2.48</sup> (0.5463)	sp <sup>1.83</sup> (0.8376)	sp <sup>1.98</sup> (0.5752)	sp <sup>1.19</sup> (0.8180)	sp <sup>99.99</sup> (0.5058)	sp <sup>99.99</sup> (0.8626)
	B3LYP/6-31G*	sp <sup>2.52</sup> (0.5539)	sp <sup>2.00</sup> (0.8326)	sp <sup>2.02</sup> (0.5812)	sp <sup>1.38</sup> (0.8138)	sp <sup>99.99</sup> (0.5405)	sp <sup>99.99</sup> (0.8414)
DMSO	HF/3-21G*	sp <sup>2.66</sup> (0.5479)	sp <sup>1.94</sup> (0.8365)	sp <sup>2.07</sup> (0.5731)	sp <sup>1.26</sup> (0.8195)	sp <sup>1.00</sup> (0.5448)	sp <sup>1.00</sup> (0.8386)
	B3LYP/3-21G*	sp <sup>2.63</sup> (0.5608)	sp <sup>2.20</sup> (0.8280)	sp <sup>2.12</sup> (0.5814)	sp <sup>1.57</sup> (0.8136)	sp <sup>99.99</sup> (0.5669)	sp <sup>99.99</sup> (0.8238)
	MP2/3-21G*	sp <sup>2.67</sup> (0.5565)	sp <sup>2.39</sup> (0.8308)	sp <sup>2.08</sup> (0.5777)	sp <sup>1.58</sup> (0.8163)	sp <sup>1.00</sup> (0.5802)	sp <sup>99.99</sup> (0.8145)
	HF/6-31G*	sp <sup>2.48</sup> (0.5463)	sp <sup>1.83</sup> (0.8376)	sp <sup>1.98</sup> (0.5752)	sp <sup>1.20</sup> (0.8180)	sp <sup>99.99</sup> (0.5060)	sp <sup>99.99</sup> (0.8625)
	B3LYP/6-31G*	sp <sup>2.52</sup> (0.5540)	sp <sup>2.00</sup> (0.8325)	sp <sup>2.02</sup> (0.5812)	sp <sup>1.38</sup> (0.8137)	sp <sup>99.99</sup> (0.5407)	sp <sup>99.99</sup> (0.8412)
H <sub>2</sub> O	HF/3-21G*	sp <sup>2.64</sup> (0.5481)	sp <sup>1.94</sup> (0.8364)	sp <sup>2.07</sup> (0.5732)	sp <sup>1.26</sup> (0.8194)	sp <sup>1.00</sup> (0.5450)	sp <sup>1.00</sup> (0.8385)
	B3LYP/3-21G*	sp <sup>2.63</sup> (0.5608)	sp <sup>2.20</sup> (0.8279)	sp <sup>2.12</sup> (0.5814)	sp <sup>1.57</sup> (0.8136)	sp <sup>99.99</sup> (0.5669)	sp <sup>99.99</sup> (0.8238)
	MP2/3-21G*	sp <sup>2.67</sup> (0.5566)	sp <sup>2.39</sup> (0.8308)	sp <sup>2.08</sup> (0.5777)	sp <sup>1.58</sup> (0.8163)	sp <sup>1.00</sup> (0.5802)	sp <sup>99.99</sup> (0.8145)
	HF/6-31G*	sp <sup>2.48</sup> (0.5463)	sp <sup>1.83</sup> (0.8376)	sp <sup>1.98</sup> (0.5752)	sp <sup>1.20</sup> (0.8180)	sp <sup>99.99</sup> (0.5060)	sp <sup>99.99</sup> (0.8625)
	B3LYP/6-31G*	sp <sup>2.51</sup> (0.5541)	sp <sup>2.00</sup> (0.8324)	sp <sup>2.01</sup> (0.5813)	sp <sup>1.38</sup> (0.8137)	sp <sup>99.99</sup> (0.5408)	sp <sup>99.99</sup> (0.8411)

**Table 3** Calculated NHOs and the polarization coefficient for each hybrid in the corresponding NBO (in parentheses) for fAla-tRNA.

Phase	Method	O <sub>30</sub> —C <sub>44</sub>		C <sub>44</sub> —O <sub>47</sub>		C <sub>44</sub> —O <sub>47</sub>	
		O <sub>30</sub>	C <sub>44</sub>	C <sub>44</sub>	O <sub>47</sub>	O <sub>30</sub>	C <sub>44</sub>
Gas	HF/3-21G*	sp <sup>1.99</sup> (0.8363)	sp <sup>2.67</sup> (0.5482)	sp <sup>2.04</sup> (0.5730)	sp <sup>1.24</sup> (0.8196)	sp <sup>1.00</sup> (0.5506)	sp <sup>1.00</sup> (0.8348)
	B3LYP/3-21G*	sp <sup>2.40</sup> (0.8277)	sp <sup>2.70</sup> (0.5611)	sp <sup>2.05</sup> (0.5794)	sp <sup>1.46</sup> (0.8151)	sp <sup>99.99</sup> (0.5821)	sp <sup>99.99</sup> (0.8131)
	MP2/3-21G*	sp <sup>2.48</sup> (0.8315)	sp <sup>2.74</sup> (0.5555)	sp <sup>2.00</sup> (0.5779)	sp <sup>1.45</sup> (0.8161)	sp <sup>99.99</sup> (0.5474)	sp <sup>1.00</sup> (0.8369)
	HF/6-31G*	sp <sup>1.94</sup> (0.8354)	sp <sup>2.61</sup> (0.5496)	sp <sup>1.99</sup> (0.5823)	sp <sup>1.39</sup> (0.8130)	sp <sup>99.99</sup> (0.5305)	sp <sup>99.99</sup> (0.8477)
	B3LYP/6-31G*	sp <sup>2.20</sup> (0.8304)	sp <sup>2.65</sup> (0.5571)	sp <sup>2.01</sup> (0.5861)	sp <sup>1.57</sup> (0.8102)	sp <sup>1.00</sup> (0.5630)	sp <sup>1.00</sup> (0.8264)
CHCl <sub>3</sub>	HF/3-21G*	sp <sup>2.02</sup> (0.8351)	sp <sup>2.64</sup> (0.5501)	sp <sup>2.04</sup> (0.5728)	sp <sup>1.24</sup> (0.8197)	sp <sup>1.00</sup> (0.5489)	sp <sup>1.00</sup> (0.8359)
	B3LYP/3-21G*	sp <sup>2.44</sup> (0.8262)	sp <sup>2.67</sup> (0.5634)	sp <sup>2.05</sup> (0.5792)	sp <sup>1.45</sup> (0.8152)	sp <sup>99.99</sup> (0.5806)	sp <sup>99.99</sup> (0.8142)
	MP2/3-21G*	sp <sup>2.64</sup> (0.8303)	sp <sup>2.75</sup> (0.5573)	sp <sup>2.04</sup> (0.5759)	sp <sup>1.51</sup> (0.8175)	sp <sup>99.99</sup> (0.5897)	sp <sup>1.00</sup> (0.8076)
	HF/6-31G*	sp <sup>1.88</sup> (0.8385)	sp <sup>2.49</sup> (0.5449)	sp <sup>1.94</sup> (0.5752)	sp <sup>1.17</sup> (0.8180)	sp <sup>99.99</sup> (0.5187)	sp <sup>99.99</sup> (0.8550)
	B3LYP/6-31G*	sp <sup>2.06</sup> (0.8329)	sp <sup>2.53</sup> (0.5534)	sp <sup>1.95</sup> (0.5816)	sp <sup>1.34</sup> (0.8135)	sp <sup>1.00</sup> (0.5517)	sp <sup>99.99</sup> (0.8340)
DMSO	HF/3-21G*	sp <sup>2.03</sup> (0.8343)	sp <sup>2.63</sup> (0.5514)	sp <sup>2.04</sup> (0.5726)	sp <sup>1.23</sup> (0.8198)	sp <sup>1.00</sup> (0.5478)	sp <sup>1.00</sup> (0.8366)
	B3LYP/3-21G*	sp <sup>2.45</sup> (0.8259)	sp <sup>2.66</sup> (0.5638)	sp <sup>2.05</sup> (0.5791)	sp <sup>1.45</sup> (0.8152)	sp <sup>99.99</sup> (0.5804)	sp <sup>99.99</sup> (0.8144)
	MP2/3-21G*	sp <sup>2.67</sup> (0.8290)	sp <sup>2.72</sup> (0.5593)	sp <sup>2.04</sup> (0.5757)	sp <sup>1.51</sup> (0.8176)	sp <sup>99.99</sup> (0.5886)	sp <sup>1.00</sup> (0.8084)
	HF/6-31G*	sp <sup>1.89</sup> (0.8379)	sp <sup>2.48</sup> (0.5458)	sp <sup>1.94</sup> (0.5750)	sp <sup>1.17</sup> (0.8181)	sp <sup>99.99</sup> (0.5170)	sp <sup>99.99</sup> (0.8560)
	B3LYP/6-31G*	sp <sup>2.08</sup> (0.8321)	sp <sup>2.51</sup> (0.5546)	sp <sup>1.95</sup> (0.5815)	sp <sup>1.34</sup> (0.8136)	sp <sup>1.00</sup> (0.5509)	sp <sup>99.99</sup> (0.8346)
H <sub>2</sub> O	HF/3-21G*	sp <sup>2.03</sup> (0.8346)	sp <sup>2.63</sup> (0.5508)	sp <sup>2.04</sup> (0.5727)	sp <sup>1.24</sup> (0.8198)	sp <sup>1.00</sup> (0.5483)	sp <sup>1.00</sup> (0.8363)
	B3LYP/3-21G*	sp <sup>2.44</sup> (0.8263)	sp <sup>2.67</sup> (0.5633)	sp <sup>2.05</sup> (0.5792)	sp <sup>1.45</sup> (0.8152)	sp <sup>99.99</sup> (0.5807)	sp <sup>99.99</sup> (0.8141)
	MP2/3-21G*	sp <sup>2.64</sup> (0.8303)	sp <sup>2.75</sup> (0.5573)	sp <sup>2.04</sup> (0.5759)	sp <sup>1.51</sup> (0.8175)	sp <sup>99.99</sup> (0.5897)	sp <sup>1.00</sup> (0.8076)
	HF/6-31G*	sp <sup>1.89</sup> (0.8381)	sp <sup>2.48</sup> (0.5455)	sp <sup>1.94</sup> (0.5751)	sp <sup>1.17</sup> (0.8181)	sp <sup>99.99</sup> (0.5181)	sp <sup>99.99</sup> (0.8553)
	B3LYP/6-31G*	sp <sup>2.07</sup> (0.8322)	sp <sup>2.51</sup> (0.5545)	sp <sup>1.95</sup> (0.5815)	sp <sup>1.34</sup> (0.8136)	sp <sup>1.00</sup> (0.5510)	sp <sup>99.99</sup> (0.8345)

the electron distribution in compounds of high ionic character (Srinivasa Rao et al., 2008).

The last section allows to quickly identify the principal delocalizing acceptor orbitals associated with each donor NBO, and their topological relationship to this NBO (see Table 6).

### 3.3. NMR parameters

Nuclear magnetic resonance (NMR) spectroscopy is a powerful tool for the structure determination of large molecules, particularly proteins in solution. The NMR technique is based on the sensitivity of magnetic properties (Czink et al., 2007). The cal-

**Table 4** Second order perturbation theory analysis of Fock matrix in NBO basis threshold for printing: 0.50 kcal/mol for fMet-tRNA and fAla-tRNA.

Phase	Method	fMet-tRNA			fAla-tRNA		
		Donor NBO ( <i>i</i> )	Acceptor NBO ( <i>j</i> )	<i>E</i> <sup>(2)</sup>	Donor NBO ( <i>i</i> )	Acceptor NBO ( <i>j</i> )	<i>E</i> <sup>(2)</sup>
Gas	HF/3-21G*	LP(2)O <sub>32</sub>	σ*(O <sub>29</sub> –C <sub>30</sub> )	51.40	LP(2)O <sub>47</sub>	σ*(O <sub>30</sub> –C <sub>44</sub> )	53.18
	B3LYP/3-21G*	LP(2)O <sub>32</sub>	σ*(O <sub>29</sub> –C <sub>30</sub> )	37.09	LP(2)O <sub>47</sub>	σ*(O <sub>30</sub> –C <sub>44</sub> )	41.29
	MP2/3-21G*	LP(2)O <sub>32</sub>	σ*(O <sub>29</sub> –C <sub>30</sub> )	47.23	LP(2)O <sub>47</sub>	σ*(O <sub>30</sub> –C <sub>44</sub> )	51.93
	HF/6-31G*	LP(2)O <sub>32</sub>	σ*(O <sub>29</sub> –C <sub>30</sub> )	43.20	LP(2)O <sub>47</sub>	σ*(O <sub>30</sub> –C <sub>44</sub> )	45.70
	B3LYP/6-31G*	LP(2)O <sub>32</sub>	σ*(O <sub>29</sub> –C <sub>30</sub> )	31.77	LP(2)O <sub>47</sub>	σ*(O <sub>30</sub> –C <sub>44</sub> )	33.54
CHCl <sub>3</sub>	HF/3-21G*	LP(2)O <sub>32</sub>	σ*(O <sub>29</sub> –C <sub>30</sub> )	51.15	LP(2)O <sub>47</sub>	σ*(O <sub>30</sub> –C <sub>44</sub> )	52.58
	B3LYP/3-21G*	LP(2)O <sub>32</sub>	σ*(O <sub>29</sub> –C <sub>30</sub> )	37.05	LP(2)O <sub>47</sub>	σ*(O <sub>30</sub> –C <sub>44</sub> )	40.68
	MP2/3-21G*	LP(2)O <sub>32</sub>	σ*(O <sub>29</sub> –C <sub>30</sub> )	–	LP(2)O <sub>47</sub>	σ*(O <sub>30</sub> –C <sub>44</sub> )	–
	HF/6-31G*	LP(2)O <sub>32</sub>	σ*(O <sub>29</sub> –C <sub>30</sub> )	43.21	LP(2)O <sub>47</sub>	σ*(O <sub>30</sub> –C <sub>44</sub> )	45.35
	B3LYP/6-31G*	LP(2)O <sub>32</sub>	σ*(O <sub>29</sub> –C <sub>30</sub> )	31.74	LP(2)O <sub>47</sub>	σ*(O <sub>30</sub> –C <sub>44</sub> )	33.29
DMSO	HF/3-21G*	LP(2)O <sub>32</sub>	σ*(O <sub>29</sub> –C <sub>30</sub> )	51.41	LP(2)O <sub>47</sub>	σ*(O <sub>30</sub> –C <sub>44</sub> )	52.18
	B3LYP/3-21G*	LP(2)O <sub>32</sub>	σ*(O <sub>29</sub> –C <sub>30</sub> )	37.01	LP(2)O <sub>47</sub>	σ*(O <sub>30</sub> –C <sub>44</sub> )	40.57
	MP2/3-21G*	LP(2)O <sub>32</sub>	σ*(O <sub>29</sub> –C <sub>30</sub> )	–	LP(2)O <sub>47</sub>	σ*(O <sub>30</sub> –C <sub>44</sub> )	–
	HF/6-31G*	LP(2)O <sub>32</sub>	σ*(O <sub>29</sub> –C <sub>30</sub> )	43.21	LP(2)O <sub>47</sub>	σ*(O <sub>30</sub> –C <sub>44</sub> )	45.94
	B3LYP/6-31G*	LP(2)O <sub>32</sub>	σ*(O <sub>29</sub> –C <sub>30</sub> )	31.73	LP(2)O <sub>47</sub>	σ*(O <sub>30</sub> –C <sub>44</sub> )	33.34
H <sub>2</sub> O	HF/3-21G*	LP(2)O <sub>32</sub>	σ*(O <sub>29</sub> –C <sub>30</sub> )	51.39	LP(2)O <sub>47</sub>	σ*(O <sub>30</sub> –C <sub>44</sub> )	52.35
	B3LYP/3-21G*	LP(2)O <sub>32</sub>	σ*(O <sub>29</sub> –C <sub>30</sub> )	37.01	LP(2)LP(2)O <sub>47</sub>	σ*(O <sub>30</sub> –C <sub>44</sub> )	40.70
	MP2/3-21G*	LP(2)O <sub>32</sub>	σ*(O <sub>29</sub> –C <sub>30</sub> )	–	LP(2)O <sub>47</sub>	σ*(O <sub>30</sub> –C <sub>44</sub> )	–
	HF/6-31G*	LP(2)O <sub>32</sub>	σ*(O <sub>29</sub> –C <sub>30</sub> )	43.21	LP(2)O <sub>47</sub>	σ*(O <sub>30</sub> –C <sub>44</sub> )	45.19
	B3LYP/6-31G*	LP(2)O <sub>32</sub>	σ*(O <sub>29</sub> –C <sub>30</sub> )	31.73	LP(2)O <sub>47</sub>	σ*(O <sub>30</sub> –C <sub>44</sub> )	33.36

**Table 5** The atomic charge distribution in terms of NPA for fMet-tRNA and fAla-tRNA.

Phase	Method	fMet-tRNA			fAla-tRNA		
		O <sub>29</sub>	C <sub>30</sub>	O <sub>32</sub>	O <sub>30</sub>	C <sub>44</sub>	O <sub>47</sub>
Gas	HF/3-21G*	-0.6361	0.9439	-0.6402	-0.6403	0.9405	-0.6223
	B3LYP/3-21G*	-0.4909	0.7566	-0.5520	-0.5174	0.7556	-0.5073
	MP2/3-21G*	-0.6170	0.9303	-0.6598	-0.6287	0.9229	-0.6145
	HF/6-31G*	-0.6487	1.0145	-0.7284	-0.6635	1.0043	-0.6884
	B3LYP/6-31G*	-0.5476	0.8491	-0.6289	-0.5641	0.8450	-0.5892
CHCl <sub>3</sub>	HF/3-21G*	-0.6367	0.9428	-0.6381	-0.6386	0.9420	-0.6277
	B3LYP/3-21G*	-0.4912	0.7557	-0.5506	-0.5137	0.7551	-0.5139
	MP2/3-21G*	-0.4936	0.72401	-0.4992	-0.5189	0.7280	-0.4593
	HF/6-31G*	-0.6491	1.0141	-0.7273	-0.6616	1.0058	-0.6926
	B3LYP/6-31G*	-0.5478	0.8486	-0.6279	-0.5614	0.8451	-0.5930
DMSO	HF/3-21G*	-0.6370	0.9425	-0.6373	-0.6375	0.9429	-0.6311
	B3LYP/3-21G*	-0.49142	0.7549	-0.5494	-0.5132	0.7549	-0.5150
	MP2/3-21G*	-0.4936	0.7240	-0.4992	-0.5189	0.7280	-0.4599
	HF/6-31G*	-0.6493	1.0138	-0.7267	-0.6589	1.0091	-0.6985
	B3LYP/6-31G*	-0.5479	0.8483	-0.6274	-0.5581	0.8455	-0.5980
H <sub>2</sub> O	HF/3-21G*	-0.6371	0.9423	-0.6369	-0.6380	0.9425	-0.6296
	B3LYP/3-21G*	-0.4914	0.7548	-0.5493	-0.5140	0.7551	-0.5136
	MP2/3-21G*	-0.4936	0.7240	-0.4992	-0.5189	0.7280	-0.4593
	HF/6-31G*	-0.6492	1.0139	-0.7268	-0.6607	1.0064	-0.6946
	B3LYP/6-31G*	-0.5480	0.8481	-0.6270	-0.5583	0.8455	-0.5970

culation of NMR parameters using ab initio (Alam, 2002) methods has important role in the molecular structure investigation.

The quantitative knowledge of chemical shielding anisotropy (CSA) tensors is important in the context of bimolecular applications of nuclear magnetic resonance (NMR). CSA tensors provide important information on the orientation of

molecular fragments and on the electronic environment of the nuclei, which depends on the molecular geometry (Scheurer et al., 1999).

The isotropic chemical shielding,  $\sigma_{\text{iso}}$ , is defined as:

$$\sigma_{\text{iso}} = (\sigma_{xx} + \sigma_{yy} + \sigma_{zz})/3 \quad (4)$$

**Table 6** Occupancy and energy (kcal/mol) for  $\sigma(O_{29}-C_{30})$  atoms from fMet-tRNA structure and  $\sigma(O_{30}-C_{44})$  atoms from fAla-tRNA structure.

Phase	Method	fMet-tRNA			fAla-tRNA		
		NBO	Occupancy	Energy	NBO	Occupancy	Energy
Gas	HF/3-21G*	$\sigma(O_{29}-C_{30})$	1.9940	-773.7255	$\sigma(O_{30}-C_{44})$	1.9934	-760.8992
	B3LYP/3-21G*	$\sigma(O_{29}-C_{30})$	1.9930	-605.5906	$\sigma(O_{30}-C_{44})$	1.9909	-568.1534
	MP2/3-21G*	$\sigma(O_{29}-C_{30})$	1.9931	-747.9600	$\sigma(O_{30}-C_{44})$	1.9913	-708.1758
	HF/6-31G*	$\sigma(O_{29}-C_{30})$	1.9921	-796.5668	$\sigma(O_{30}-C_{44})$	1.9920	-776.7438
	B3LYP/6-31G*	$\sigma(O_{29}-C_{30})$	1.9918	-606.8519	$\sigma(O_{30}-C_{44})$	1.9913	-588.2086
CHCl <sub>3</sub>	HF/3-21G*	$\sigma(O_{29}-C_{30})$	1.9940	-773.8447	$\sigma(O_{30}-C_{44})$	1.9934	-764.6517
	B3LYP/3-21G*	$\sigma(O_{29}-C_{30})$	1.9931	-605.9985	$\sigma(O_{30}-C_{44})$	1.9910	-574.0708
	MP2/3-21G*	$\sigma(O_{29}-C_{30})$	1.9659	-	$\sigma(O_{30}-C_{44})$	1.9629	-
	HF/6-31G*	$\sigma(O_{29}-C_{30})$	1.9921	-796.6045	$\sigma(O_{30}-C_{44})$	1.9782	-519.4649
	B3LYP/6-31G*	$\sigma(O_{29}-C_{30})$	1.9918	-607.2033	$\sigma(O_{30}-C_{44})$	1.9913	-591.4214
DMSO	HF/3-21G*	$\sigma(O_{29}-C_{30})$	1.9940	-774.0643	$\sigma(O_{30}-C_{44})$	1.9934	-767.2245
	B3LYP/3-21G*	$\sigma(O_{29}-C_{30})$	1.9931	-606.3248	$\sigma(O_{30}-C_{44})$	1.9910	-575.2003
	MP2/3-21G*	$\sigma(O_{29}-C_{30})$	1.9658	-	$\sigma(O_{30}-C_{44})$	1.9629	-
	HF/6-31G*	$\sigma(O_{29}-C_{30})$	1.9921	-796.6170	$\sigma(O_{30}-C_{44})$	1.9917	-780.3269
	B3LYP/6-31G*	$\sigma(O_{29}-C_{30})$	1.9918	-607.3853	$\sigma(O_{30}-C_{44})$	1.9911	-593.8562
H <sub>2</sub> O	HF/3-21G*	$\sigma(O_{29}-C_{30})$	1.9940	-774.1773	$\sigma(O_{30}-C_{44})$	1.9934	-766.1012
	B3LYP/3-21G*	$\sigma(O_{29}-C_{30})$	1.9931	-606.3562	$\sigma(O_{30}-C_{44})$	1.9910	-573.8449
	MP2/3-21G*	$\sigma(O_{29}-C_{30})$	1.9658	-	$\sigma(O_{30}-C_{44})$	1.9628	-
	HF/6-31G*	$\sigma(O_{29}-C_{30})$	1.9921	-796.6170	$\sigma(O_{30}-C_{44})$	1.9919	-780.6657
	B3LYP/6-31G*	$\sigma(O_{29}-C_{30})$	1.9918	-607.5233	$\sigma(O_{30}-C_{44})$	1.9911	-593.5299

**Table 7** NMR parameters for fMet-tRNA.

Method	Atom	$\sigma_{iso}$ (ppm)	$\sigma_{33}$ (ppm)	$\sigma_{22}$ (ppm)	$\sigma_{11}$ (ppm)	$\gamma\sigma$ (ppm)	$\dot{E}$ (ppm)
HF/3-21G*	O <sub>29</sub>	221.10	284.18	135.05	244.06	94.63	-1.73
	C <sub>30</sub>	44.28	50.38	85.56	-3.0947	9.15	14.54
	O <sub>32</sub>	-50.78	-62.69	-34.75	-54.88	-6.16	-6.80
B3LYP/3-21G*	O <sub>29</sub>	137.08	155.57	120.48	135.18	27.73	-0.80
	C <sub>30</sub>	36.13	38.44	54.52	15.44	3.45	16.97
	O <sub>32</sub>	-46.02	-259.11	118.82	2.24	72.38	7.83
HF/6-31G*	O <sub>29</sub>	198.67	199.38	208.30	188.32	1.07	28.03
	C <sub>30</sub>	33.34	26.94	72.58	0.48	-9.59	-11.28
	O <sub>32</sub>	-8.50	-235.39	231.81	-21.90	-20.11	-34.84
B3LYP/6-31G*	O <sub>29</sub>	125.34	107.72	144.77	123.54	-2.70	-20.56
	C <sub>30</sub>	21.72	28.22	39.75	-2.81	9.75	6.55
	O <sub>32</sub>	-36.57	-256.90	157.35	-10.15	39.62	15.68

**Table 8** NMR parameters for fAla-tRNA.

Method	atom	$\sigma_{iso}$ (ppm)	$\sigma_{33}$ (ppm)	$\sigma_{22}$ (ppm)	$\sigma_{11}$ (ppm)	$\gamma\sigma$ (ppm)	$\dot{E}$ (ppm)
HF/3-21G*	O <sub>30</sub>	225.45	170.47	244.56	261.32	53.80	2.07
	C <sub>44</sub>	46.39	80.76	79.98	-21.59	51.59	2.95
	O <sub>47</sub>	-63.70	-274.28	210.89	-127.70	-96.01	-7.58
B3LYP/3-21G*	O <sub>30</sub>	159.09	93.22	195.71	188.34	43.87	3.50
	C <sub>44</sub>	39.83	74.22	62.23	-16.954	51.58	2.30
	O <sub>47</sub>	-69.40	-294.37	199.03	-112.85	-65.18	-11.35
HF/6-31G*	O <sub>30</sub>	206.44	144.76	245.60	228.98	33.80	4.48
	C <sub>44</sub>	37.61	66.60	88.63	-42.39	43.48	4.52
	O <sub>47</sub>	-22.87	-223.21	304.69	-150.09	-190.83	-4.15
B3LYP/6-31G*	O <sub>30</sub>	141.60	72.08	199.55	153.18	17.37	11.01
	C <sub>44</sub>	26.31	58.38	72.50	-51.94	48.10	3.88
	O <sub>47</sub>	-46.18	-258.27	292.96	-173.24	-190.58	-4.34

The chemical shielding anisotropy,  $\Psi\sigma$ , and asymmetry parameter of the chemical shielding,  $\dot{E}$ , are given by:

When  $\sigma_{zz} - \sigma_{iso} > \sigma_{xx} - \sigma_{iso}$

$$\Psi\sigma = \sigma_{zz} - 1/2(\sigma_{yy} + \sigma_{xx}) \quad (5)$$

$$\dot{E} = \sigma_{yy} - \sigma_{zz}/\sigma_{xx} - \sigma_{iso} \quad (6)$$

When  $\sigma_{zz} - \sigma_{iso} < \sigma_{xx} - \sigma_{iso}$

$$\Psi\sigma = \sigma_{xx} - 1/2(\sigma_{yy} + \sigma_{zz}) \quad (7)$$

$$\dot{E} = \sigma_{yy} - \sigma_{zz}/\sigma_{xx} - \sigma_{iso} \quad (8)$$

The calculations of NMR shielding tensors were done (Infante-Castillo and Hernandez-Rivera, 2010) at the HF and B3LYP levels of theory using input of the optimized structure at every method in gas phase. Tables 7 and 8 show the  $\sigma_{xx}$ ,  $\sigma_{yy}$ ,  $\sigma_{zz}$ ,  $\sigma_{iso}$ ,  $\dot{E}$ , and  $\Psi\sigma$  values for atoms in the area link in the fMet-tRNA and fAla-tRNA structures.

**Table 9** Thermochemistry values for fMet-tRNA at 298.15 K and 1.00 atmosphere pressure.

Phase	Methods	$E_{ZPE}$	$E_{tot}$	$H_{corr}$	$G_{corr}$	$\varepsilon_0 + E_{ZPE}$	$\varepsilon_0 + E_{tot}$	$\varepsilon_0 + H_{corr}$	$\varepsilon_0 + G_{corr}$
Gas	HF/3-21G*	290.71	310.06	310.65	248.82	-1471662.49	-1471643.15	-1471642.55	-1471704.39
	B3lyp/3-21G*	269.36	289.57	290.16	226.96	-1478347.44	-1478327.22	-1478326.63	-1478389.84
CHCl <sub>3</sub>	HF/3-21G*	290.63	309.99	310.59	248.73	-1471663.08	-1471643.71	-1471643.12	-1471704.98
	B3lyp/3-21G*	269.29	289.52	290.11	226.83	-1478347.91	-1478327.67	-1478327.08	-1478390.36
DMSO	HF/3-21G*	290.60	309.96	310.56	248.68	-1471663.34	-1471643.97	-1471643.37	-1471705.25
	B3lyp/3-21G*	269.23	289.47	290.06	226.70	-1478348.29	-1478328.04	-1478327.45	-1478390.81
H <sub>2</sub> O	HF/3-21G*	290.58	309.95	310.54	248.66	-1471663.47	-1471644.10	-1471643.50	-1471705.40
	B3lyp/3-21G*	269.28	289.50	290.09	226.99	-1478348.27	-1478328.05	-1478327.46	-1478390.56
<hr/>									
Gas		$E_{tot(Thermal)}$	$(C_v)_{tot}$	$S_{tot}$	$Q_{tot}$ BOT	$Q_{tot} V = 0$	$\ln(Q)_{tot}$ BOT	$\ln(Q)_{tot} V = 0$	
	HF/3-21G*	310.06	112.75	207.39	0.41E-182	0.51E+31	-419.95	70.71	
CHCl <sub>3</sub>	HF/3-21G*	289.57	120.06	212.00	0.43E-166	0.12E+32	-383.06	71.56	
	B3lyp/3-21G*	289.52	120.11	212.23	0.53E-166	0.13E+32	-382.85	71.65	
DMSO	HF/3-21G*	309.99	112.79	207.45	0.47E-182	0.51E+31	-419.82	70.71	
	B3lyp/3-21G*	289.52	120.11	212.23	0.53E-166	0.13E+32	-382.85	71.65	
H <sub>2</sub> O	HF/3-21G*	309.96	112.82	207.52	0.51E-182	0.52E+31	-419.73	70.73	
	B3lyp/3-21G*	289.47	120.15	212.51	0.66E-166	0.14E+32	-382.63	71.76	
		$E_{tot(Thermal)}$	$(C_v)_{tot}$	$S_{tot}$	$Q_{tot}$ BOT	$Q_{tot} V = 0$	$\ln(Q)_{tot}$ BOT	$\ln(Q)_{tot} V = 0$	
	HF/3-21G*	309.95	112.83	207.56	0.53E-182	0.53E+31	-419.68	70.75	
	B3lyp/3-21G*	289.50	120.11	211.62	0.40E-166	0.99E+31	-383.13	71.37	

**Table 10** Thermochemistry values for fMet-tRNA at 310.15 K and 1.00 atmosphere pressure.

Phase	Methods	$E_{ZPE}$	$E_{tot}$	$H_{corr}$	$G_{corr}$	$\varepsilon_0 + E_{ZPE}$	$\varepsilon_0 + E_{tot}$	$\varepsilon_0 + H_{corr}$	$\varepsilon_0 + G_{corr}$
Gas	HF/3-21G*	290.63	311.37	311.98	246.22	-1471663.08	-1471642.34	-1471641.73	-1471707.49
	B3lyp/3-21G*	269.42	291.07	291.68	224.68	-1478347.31	-1478325.67	-1478325.05	-1478392.05
CHCl <sub>3</sub>	HF/3-21G*	290.63	311.37	311.98	246.22	-1471663.08	-1471642.34	-1471641.73	-1471707.49
	B3lyp/3-21G*	269.28	290.96	291.58	224.43	-1478348.27	-1478326.59	-1478325.97	-1478393.13
DMSO	HF/3-21G*	290.60	311.34	311.96	246.17	-1471663.34	-1471642.6	-1471641.98	-1471707.77
	B3lyp/3-21G*	269.28	290.96	291.58	224.43	-1478348.27	-1478326.59	-1478325.97	-1478393.13
H <sub>2</sub> O	HF/3-21G*	290.58	311.32	311.94	246.14	-1471663.47	-1471642.73	-1471642.11	-1471707.91
	B3lyp/3-21G*	269.28	290.96	291.58	224.43	-1478348.27	-1478326.59	-1478325.97	-1478393.13
<hr/>									
Gas		$E_{tot(Thermal)}$	$(C_v)_{tot}$	$S_{tot}$	$Q_{tot}$ BOT	$Q_{tot} V = 0$	$\ln(Q)_{tot}$ BOT	$\ln(Q)_{tot} V = 0$	
	HF/3-21G*	311.37	116.48	212.05	0.31E-173	0.19E+32	-399.49	72.06	
CHCl <sub>3</sub>	HF/3-21G*	291.07	124.02	216.01	0.47E-158	0.33E+32	-364.55	72.57	
	B3lyp/3-21G*	290.96	124.12	216.51	0.71E-158	0.40E+32	-364.13	72.77	
DMSO	HF/3-21G*	311.37	116.48	212.05	0.31E-173	0.19E+32	-399.49	72.06	
	B3lyp/3-21G*	290.96	124.12	216.51	0.71E-158	0.40E+32	-364.13	72.77	
H <sub>2</sub> O	HF/3-21G*	311.33	116.52	212.17	0.36E-173	0.20E+32	-399.36	72.10	
	B3lyp/3-21G*	290.96	124.12	216.51	0.71E-158	0.40E+32	-364.13	72.77	

In the Tables 10 and 11 the numbers of  $\gamma\sigma$  and  $\dot{E}$  that are not bold follow the rule of  $\sigma_{zz} - \sigma_{iso} > \sigma_{xx} - \sigma_{iso}$  and other numbers that are bold follow the rule of  $\sigma_{zz} - \sigma_{iso} < \sigma_{xx} - \sigma_{iso}$ .

The asymmetry parameter of the chemical shielding,  $\dot{E}$ , and the chemical shielding anisotropy,  $\gamma\sigma$ , of electrons of the connection area, in several methods, are obtained differently. This is due to  $\sigma_{xx}$ ,  $\sigma_{yy}$ ,  $\sigma_{zz}$ ,  $\sigma_{iso}$  values for both structures that have been obtained differently.

### 3.4. Frequency calculations

The vibrational frequencies of fMet-tRNA and fAla-tRNA were calculated at the Hartree–Fock (HF), DFT (B3LYP) levels of theory using the 3-21G\* basis set (Jensen, 2003). The entropies and heat capacities were calculated using statistical mechanics based on the vibrational frequencies (Zheng et al., 2005). The nature of all stationary point structures were

**Table 11** Thermochemistry values for fAla-tRNA at 298.15 K and 1.00 atmosphere pressure.

Phase	Methods	$E_{ZPE}$	$E_{tot}$	$H_{corr}$	$G_{corr}$	$\varepsilon_0 + E_{ZPE}$	$\varepsilon_0 + E_{tot}$	$\varepsilon_0 + H_{corr}$	$\varepsilon_0 + G_{corr}$
Gas	HF/3-21G*	251.53	268.06	268.65	214.25	−1174696.01	−1174680.99	−1174679.24	−1174734.98
	B3lyp/3-21G*	232.25	249.74	250.33	194.14	−1180604.11	−1180587.34	−1180586.00	−1180643.51
CHCl <sub>3</sub>	HF/3-21G*	251.48	268.01	268.60	214.28	−1174699.05	−1174683.21	−1174682.56	−1174736.33
	B3lyp/3-21G*	232.25	249.70	250.30	194.40	−1180607.45	−1180590.11	−1180589.34	−1180645.10
DMSO	HF/3-21G*	251.46	267.99	268.58	214.24	−1174700.46	−1174684.12	−1174683.25	−1174737.09
	B3lyp/3-21G*	232.25	249.69	250.28	194.40	−1180608.22	−1180591.68	−1180590.66	−1180646.01
H <sub>2</sub> O	HF/3-21G*	251.46	267.99	268.58	214.24	−1174700.13	−1174684.16	−1174683.14	−1174737.67
	B3lyp/3-21G*	232.26	249.70	250.30	194.40	−1180607.23	−1180590.46	−1180589.18	−1180645.44
<hr/>									
Gas		$E_{tot(Thermal)}$	$(C_v)_{tot}$	$S_{tot}$	$Q_{tot}$ BOT	$Q_{tot} V = 0$	$\ln(Q)_{tot}$ BOT	$\ln(Q)_{tot} V = 0$	
	HF/3-21G*	268.06	98.13	182.45	0.88E−157	0.21E+28	361.62−	62.91	
CHCl <sub>3</sub>	B3lyp/3-21G*	249.74	104.91	188.47	0.49E−142	0.87E+28	327.67−	64.33	
	HF/3-21G*	268.01	98.14	182.19	0.84E−157	0.18E+28	−361.67	62.78	
DMSO	B3lyp/3-21G*	249.70	104.89	187.46	0.31E−142	0.55E+28	−328.11	63.88	
	HF/3-21G*	267.99	98.15	182.25	0.90E−157	0.19E+28	−361.60	62.81	
H <sub>2</sub> O	B3lyp/3-21G*	249.69	104.89	187.43	0.31E−142	0.55E+28	−328.11	63.87	
	HF/3-21G*	267.99	98.15	182.26	0.91E−157	0.19E+28	−361.59	62.81	
B3lyp/3-21G*	249.70	104.89	187.48	0.31E−142	0.56E+28	−328.11	63.89		

**Table 12** Thermochemistry values for fAla-tRNA at 310.15 K 1.00 atmosphere pressure.

Phase	Methods	$E_{ZPE}$	$E_{tot}$	$H_{corr}$	$G_{corr}$	$\varepsilon_0 + E_{ZPE}$	$\varepsilon_0 + E_{tot}$	$\varepsilon_0 + H_{corr}$	$\varepsilon_0 + G_{corr}$
Gas	HF/3-21G*	251.53	269.26	269.87	212.04	−1174696.46	−1174678.73	−1174678.11	−1174735.94
	B3lyp/3-21G*	232.25	251.02	251.63	191.85	−1180603.91	−1180585.14	−1180584.53	−1180644.31
CHCl <sub>3</sub>	HF/3-21G*	251.48	269.21	269.82	212.07	−1174699.10	−1174681.38	−1174680.76	−1174738.51
	B3lyp/3-21G*	232.25	250.98	251.60	192.13	−1180607.37	−1180588.64	−1180588.02	−1180647.5
DMSO	HF/3-21G*	251.46	269.19	269.80	212.03	−1174700.17	−1174682.44	−1174681.82	−1174739.59
	B3lyp/3-21G*	232.25	250.97	251.59	192.13	−1180608.02	−1180589.29	−1180588.68	−1180648.14
H <sub>2</sub> O	HF/3-21G*	251.46	269.18	269.80	212.03	−1174700.22	−1174682.49	−1174681.88	−1174739.65
	B3lyp/3-21G*	232.26	250.98	251.60	192.12	−1180607.24	−1180588.51	−1180587.89	−1180647.37
<hr/>									
Gas		$E_{tot(Thermal)}$	$(C_v)_{tot}$	$S_{tot}$	$Q_{tot}$ BOT	$Q_{tot} V = 0$	$\ln(Q)_{tot}$ BOT	$\ln(Q)_{tot} V = 0$	
	HF/3-21G*	269.26	101.45	186.47	0.38E−149	0.66E+28	−344.04	64.07	
CHCl <sub>3</sub>	B3lyp/3-21G*	251.02	108.48	192.76	0.648E−135	0.29E+29	−311.28	65.55	
	HF/3-21G*	269.21	101.47	186.21	0.365E−149	0.59E+28	−344.09	63.94	
DMSO	B3lyp/3-21G*	250.98	108.47	191.75	0.41E−135	0.18E+29	−311.73	65.10	
	HF/3-21G*	269.19	101.48	186.27	0.39E−149	0.60E+28	−344.02	63.97	
H <sub>2</sub> O	B3lyp/3-21G*	250.97	108.47	191.71	0.41E−135	0.18E+29	−311.73	65.09	
	HF/3-21G*	269.18	101.48	186.28	0.39E−149	0.60E+28	−344.01	63.97	
B3lyp/3-21G*	250.98	108.47	191.76	0.41E−135	0.18E+29	−311.72	65.11		

determined by analytical frequency analysis, which also provided zero-point vibrational energies (ZPEs) Cherkaoui and Boutalib, 2006. Electronic energies, enthalpies, Gibbs free energies and zero point vibrational energies for both the compounds using frequency calculation at 298.15 K and 310.15 K temperatures are presented in Tables 9–12. Thermochemistry analysis follows the frequency and normal mode data.

$$E_{\text{tot}} = E_t + E_r + E_v + E_e$$

$$H_{\text{corr}} = E_{\text{tot}} + k_B T$$

$$G_{\text{corr}} = H_{\text{corr}} - T_{\text{stot}}$$

$$S_{\text{tot}} = S_t + S_r + S_v + S_e$$

$$\text{Sum of electronic and zero-point energies} = \mathcal{E}_0 + E_{\text{ZPE}}$$

$$\text{Sum of electronic and thermal energies} = \mathcal{E}_0 + E_{\text{tot}}$$

$$\text{Sum of electronic and thermal enthalpies} = \mathcal{E}_0 + H_{\text{corr}}$$

$$\text{Sum of electronic and thermal free energies} = \mathcal{E}_0 + G_{\text{corr}}$$

where  $\mathcal{E}_0$  is the total electronic energy at  $T = 0$  K,  $G_{\text{corr}}$  and  $H_{\text{corr}}$  represent the thermal correction to Gibbs free energy and enthalpy, respectively. The internal thermal energy  $E_{\text{tot}}$  is contributed from translational ( $E_t$ ), rotational ( $E_r$ ), vibrational ( $E_v$ ), and electronic ( $E_e$ ) energies, and  $S_{\text{tot}}$ ,  $S_t$ ,  $S_r$ ,  $S_v$ ,  $S_e$  are the corresponding entropies (An et al., 2005). The next section is the individual contribution to the internal thermal energy ( $E_{\text{tot}}$ ), constant volume molar heat capacity ( $C_v$ )<sub>tot</sub>, entropy ( $S_{\text{tot}}$ ) and Partition function ( $Q$ ) Ochterski, 2000.

The partition functions are also computed, with both the bottom of the vibrational well and the lowest (zero-point) vibrational state as reference.

The comparison of thermochemistry values were calculated for two structures, which show that with increasing temperature, these values increase in both structures and also these values for fMet-tRNA at two temperatures are more than fAla-tRNA which shows the greater stability of fMet-tRNA than fAla-tRNA.

#### 4. Conclusion

In the present study, we used a combination of theoretical tools to compare fMet-tRNA structure (the first amino acid required for protein synthesis) and fAla-tRNA structure (artificial amino acid). The following conclusions are obtained from the current study:

1. The most stable structure, according to the optimization energy is fMet-tRNA. Probably for this reason, it is chosen for the initiation of protein synthesis. Desired structures have their most stable state in water solvent and then in DMSO solvent that is stable which represents a direct relation of the structure stability and solvent dielectric constant.
2. NBO analysis indicated the presence of donor-acceptor centers in the investigated structures. In both the structures, the resonance energy in the gas phase is more than that in the solvent that indicates more electrons participate in the resonance of the connection area in this phase. Among the solvents for fMet-tRNA, in DMSO, and for fAla-tRNA, in CHCl<sub>3</sub>, more electrons are involved in the resonance. The comparison between the NBO analysis of two

Compounds in gas Phase and CHCl<sub>3</sub>, DMSO and H<sub>2</sub>O solvents shows that values of  $E^{(2)}$  for fMet-tRNA are lower than fAla-tRNA which means that in the fMet-tRNA structure lesser electrons are involved in the resonance.

3. By increasing method accuracy, occupancy of orbitals of the connection area atoms in fMet-tRNA decrease but in fAla-tRNA, there is no regular trend.
4. O<sub>29</sub> in the fMet-tRNA structure and O<sub>30</sub> in the fAla-tRNA structure have maximum values of the  $\sigma_{\text{iso}}$ . This means that electron density around these atoms is further. This is maximum in the HF/3-21G\* method.
5.  $\Psi\sigma$  for carbon atoms (C<sub>30</sub>, C<sub>44</sub>) is almost positive value that represents shielding effect on these atoms is high. This effect on C<sub>44</sub> atom of fAla-tRNA structure is more than that of fMet-tRNA.
6. The Comparison of thermochemistry parameters of two structures that are expressed in Tables 9–12 show that with increasing temperature, the thermal correction to Gibbs free energy and enthalpy ( $G_{\text{corr}}$ ,  $H_{\text{corr}}$ ), the internal thermal energy ( $E_{\text{tot}}$ ), constant volume molar heat capacity ( $C_v$ )<sub>tot</sub>, entropy ( $S_{\text{tot}}$ ) and the individual contributions to the internal thermal energy ( $E_{\text{tot}}$ ) increase in both structures and these parameters values for fMet-tRNA at two temperatures are more than those of fAla-tRNA which again indicates the greater stability of fMet-tRNA.
7. Finally, our studies on the structures showed that fMet-tRNA structure is more stable than fAla-tRNA structure and fAla-tRNA cannot be used instead of fMet-tRNA for the initiation of protein synthesis.

#### References

- Agirrezabal, X., Frank, J., 2009. Elongation in translation as a dynamic interaction among the ribosome, tRNA, and elongation factors EF-G and EF-Tu. *Q. Rev. Biophys.* 42 (3), 159–200.
- Alabugin, I.V., Manoharan, M., Zeidan, T.A., 2003. Homoanomeric effects in six-membered heterocycles. *J. Am. Chem. Soc.* 125, 14014–14031.
- Alam, Todd M., 2002. Ab initio calculations of 31P NMR chemical shielding anisotropy tensors in phosphates: variations due to ring formation. *Int. J. Mol. Sci.* 3, 888–906.
- An, W., Gao, Y., Bulusu, S., Zeng, X.C., 2005. Ab initio calculation of bowl, cage, and ring isomers of C20 and C20-. *J. Chem. Phys.* 122, 204109.
- Antoun, A., Pavlov, M.Y., Lovmar, M., Ehrenberg, M., 2006. How initiation factors maximize the accuracy of tRNA selection in initiation of bacterial protein synthesis. *Mol. Cell* 23, 183–193.
- Aquino, A.J.A., Tunega, D., Haberhauer, G., Gerzabek, M.H., Lischka, H., 2002. Solvent effects on hydrogen BondssA theoretical study. *J. Phys. Chem. A* 106, 1862–1871.
- Baouz, S., Woisard, A., Chenoune, L., Aguié, G., Keith, G., Schmitter, J.M., Le Caer, J.P., Hountondji, C., 2009. Recent advances in the characterization of peptidyl transferase center: zero-distance labeling of proteins at or near the catalytic site of human 80S or Escherichiacoli 70S ribosomes by means of periodate oxidized tRNA. *Afr. J. Biochem. Res.* 3, 302–311.
- Blicharska, B., Kupka, T., 2002. Theoretical DFT and experimental NMR studies on uracil and 5-fluorouracil. *J. Mol. Struct.* 613, 153–166.
- Carter, A.P., Clemons, W.M., Brodersen, D.E., Morgan-Warren, R.J., Wimberly, B.T., Ramakrishnan, V., 2000. Functional insights from the structure of the 30S ribosomal subunit and its interactions with antibiotics. *Nature* 407, 340–348.

- Chalut, C., Egly, J.M., 1995. AUC is used as a start codon in *Escherichia coli*. *Gene* 156, 43–45.
- Chamieh, H., Guetta, D., Franzetti, B., 2008. The two PAN ATPases from Halobacterium display N-terminal heterogeneity and form labile complexes with the 20S proteasome. *Biochem. J.* 411, 387–397.
- Cherkaoui, M., Boutalib, A., 2006. Ab initio investigation of the substituent effect of the alanine complexes. *Internet Electron. J. Mol. Des.* 5, 471–478.
- Chojnacki, J., 2008. DFT and NBO theoretical study of protonation of tri-tert- butoxysilanethiol and its anion. *Polyhedron* 27, 969–976.
- Chuang, Li-Yeh., Lin, Yu-Da., Yang, C-H., 2010. PtRNASS: prediction of tRNA secondary structure from nucleotide sequences. *IAENG Int. J. Comput. Sci.* 37, IJCS\_37\_3\_02.
- Czinki, E., Császár, A.G., Magyarfalvi, G., Schreiner, P.R., Allen, W.D., 2007. Predicting secondary structures of peptides and proteins via NMR chemical shielding anisotropy (CSA) parameters. *J. Am. Chem. Soc.* 129, 1568–1577.
- Feinberg, J.S., Joseph, S., 2006. A conserved base-pair between tRNA and 23 S rRNA in the peptidyl transferase center is important for peptide release. *J. Mol. Biol.* 364, 1010–1020.
- Frisch, M.J. et al., 2003. Gaussian 03, revision B03. Gaussian Inc., Pittsburgh, PA.
- Giese, B., McNaughton, D., 2002. Surface-enhanced Raman spectroscopic study of uracil. The influence of the surface substrate, surface potential, and pH. *J. Phys. Chem. B* 106, 1461–1470.
- Infante-Castillo, R., Hernandez-Rivera, S.P., 2010. On the choice of optimal protocol for calculation of 13C and 15N NMR isotropic chemical shifts in nitramine systems. *J. Mol. Struct. (Theochem)* 940, 124–128.
- Jayabharathia, J., Thanikachalam, V., Vijayan, N., Srinivasan, N., Venkatesh Perumal, M., 2010a. Optical properties of organic nonlinear optical crystal – a combined experimental and theoretical study. *Struct. Chem. Commun.* 1, 46–52.
- Jayabharathia, J., Padmavathy, M., Srinivasan, N., 2010b. DFT based characterization of some heterocyclic compounds and their biological studies. *Struct. Chem. Commun.* 1, 15–24.
- Jensen, James O., 2003. Quantum chemical analysis of the vibrational frequencies and structure of tetrachlorodiborane. *J. Mol. Struct. (Theochem)* 635, 211–219.
- Krishnan, A.R., Subashchandrabose, S., Saleem, H., Sundaraganesan, N., Erdogdu, Y., 2010. Theoretical investigations on the molecular structure, vibrational spectra, infrared, Raman, UV and NMR spectral analysis of 4-nitrothioanisole. *Struct. Chem. Commun.* 1, 56–62.
- LaPlante, A.J., Stidham, H.D., 2009. Vibrational spectrum, ab initio calculations, conformational stabilities and assignment of fundamentals of 1,2-dibromopropane. *Spectrochim. Acta A* 74, 808–818.
- Laursen, B.S., Sørensen, H.P., Mortensen, K.K., Sperling-Petersen, H.U., 2005. Initiation of protein synthesis in bacteria. *Microbiol. Mol. Biol. Rev.* 69, 101–123.
- Martin, F., Zipse, H., 2005. Charge distribution in the water molecule – a comparison of methods. *J. Comput. Chem.* 26, 97–105.
- Munro, J.B., Sanbonmatsu, K.Y., Spahn, C.M.T., Blanchard, S.C., 2009. Navigating the ribosome's metastable energy landscape. *Trends Biochem. Sci.* 34, 390–400.
- Nandini, G., Sathyaranayana, D.N., 2004. Ab initio studies of solvent effect on molecular conformation and vibrational spectra of diacetamide. *Spectrochim. Acta A* 60, 1115–1126.
- Nekoei, A.R., Tayyari, S.F., Vakili, M., Holakoei, S., Hamidian, A.H., Sammelson, R.E., 2009. Conformation and vibrational spectra and assignment of 2-thenoyl trifluoroacetone. *J. Mol. Struct.* 932, 112–122.
- Ochterski, J.W., 2000. Ph.D., Thermochemistry in Gaussian; June 2.
- Pavlov, M.Y., Antoun, A., Lovmar, M., Ehrenberg, M., 2008. Complementary roles of initiation factor 1 and ribosome recycling factor in 70S ribosome splitting. *EMBO J.* 27, 1706–1717.
- Scheurer, C., Skrynnikov, N.R., Lienin, S.F., Straus, S.K., Brulschweiler, R., Ernst, R.R., 1999. Effects of dynamics and environment on 15N chemical shielding anisotropy in proteins. A combination of density functional theory, molecular dynamics simulation, and NMR relaxation. *J. Am. Chem. Soc.* 121, 4242–4251.
- Scholtzová, E., Mach, P., Langer, V., 2009. NBO analysis – a useful tool on interpretation of results of crystal structure determination. *Acta Cryst. A* 65, s270.
- Selmer, M., Dunham, C.M., Murphy IV, F.V., Weixlbaumer, A., Petry, S., Kelley, A.C., Weir, J.R., Ramakrishnan, V., 2006. Structure of the 70S ribosome complexed with mRNA and tRNA. *Science* 313, 1935–1942.
- Spector, S., Flynn, J.M., Tidor, B., Baker, T.A., Sauer, R.T., 2003. Expression of N-formylated proteins in *Escherichia coli*. *Protein Expr. Purif.* 32, 317–322.
- Srinivasa Rao, J., Dinadayanale, T.C., Leszczynski, Jerzy, Narahari Sastry, G., 2008. Comprehensive study on the solvation of monoand divalent metal cations: Li<sup>+</sup>, Na<sup>+</sup>, K<sup>+</sup>, Be<sup>2+</sup>, Mg<sup>2+</sup> and Ca. *J. Phys. Chem. A* 112 (50), 12944–12953.
- Subashchandrabose, S., Krishnan, A.R., Saleem, H., Thanikachalam, V., Manikandan, G., Erdogdu, Y., 2010. FT-IR, FT-Raman, NMR spectral analysis and theoretical NBO, HOMO-LUMO analysis of bis (4-amino-5-mercaptop-1,2,4-triazol-3-yl)ethane by ab initio HF and DFT methods. *J. Mol. Struct.* 981, 59–70.
- Szarecka, A., Rychlewski, J., Rychlewska, U., 1998. Theoretical salvation models: Ab initio study of molecular aggregation. *Comput. Meth. Sci. Technol.* 4, 25–33.
- Tang, J., Hernandez, G., LeMaster, D.M., 2004. Increased peptide deformylase activity for N-formylmethionine processing of proteins overexpressed in *Escherichia coli*: application to homogeneous rubredoxin production. *Protein Expr. Purif.* 36, 100–105.
- Trabuco, L.G., Schreiner, E., Eargle, J., Cornish, P., Ha, Taekjip, Luthey-Schulten, Z., Schulten, K., 2010. The role of L1 Stalk-tRNA interaction in the ribosome elongation cycle. *J. Mol. Biol.* 402, 741–760.
- Wedel, T., Gehring, T., Podlech, J., Kordel, E., Bihlmeier, A., Klopper, W., 2008. Nucleophilic additions to alkylidenebisulfides – stereoelectronic effects in vinylsulfides. *Chem. A Eur. J.* 14, 4631–4639.
- Weinhold, F., Landis, C.R., 2001. Natural bond orbitals and extensions of localized bonding concepts. *Chemistry* 2, 91–104.
- Wienk, B.H., Tomaselli, S., Bernard, C., Spurio, R., Picone, D., Gualerzi, C.O., Rolf, B., 2005. Solution structure of the C1-subdomain of *Bacillus stearothermophilus* translation initiation factor IF2. *Protein Sci.* 14, 2461–2468.
- Yu Wang, Zh., Shimonaga, M., Kobayashi, M., Nozawa, T., 2002. N-terminal methylation of the core light-harvesting complex in purple photosynthetic bacteria. *FEBS Lett.* 519, 164–168.
- Yusupov, M.M., Yusupova, G.Zh., Baucom, A., Lieberman, K., Earnest, T.N., Cate, J.H.D., Noller, H.F., 2001. Crystal structure of the ribosome at 5.5 Å resolution. *Science* 292, 883–896.
- Zheng, X.L., Sun, H.Y., Law, C.K., 2005. Thermochemical and kinetic analysis on oxidation of isobutetyl radical and 2-hydroperoxyethyl-2-propenyl radical. *J. Phys. Chem. A* 109, 9044–9053.